Mechanical Properties of Laser-Deposited Ti-6Al-4V

P.A. Kobryn and S.L. Semiatin

Air Force Research Laboratory, AFRL/MLLMP,
Wright-Patterson Air Force Base, OH 45433-7817

Abstract

Laser additive manufacturing is a solid-freeform-fabrication process which is being investigated for titanium-component manufacturing and repair based on its cost-reduction potential and flexibility. Laser additive manufacturing also has the potential to improve mechanical properties due to the high cooling rates involved. However, the effect of the layered manufacturing process and any lack-of-fusion porosity and texture on the magnitude and anisotropy of mechanical properties is of concern. Hence, a preliminary effort was undertaken to assess these effects for bulk Ti-6Al-4V deposits manufactured using the LENS™ process. Tension, fatigue, and crack-growth tests were performed on both stress-relieved and HIP'ed deposits in three primary directions. The results were compared to published data for conventionally processed Ti-6Al-4V castings and forgings.

Introduction

Laser additive manufacturing is a solid-freeform-fabrication method which can be used to manufacture solid metallic components directly from CAD files. During laser additive manufacturing, powder is fed into a melt pool which is produced by a sharply-focused laser beam. Parts are built in a layer-by-layer fashion by rastering the laser and powder source across the substrate. Laser additive manufacturing has many potential applications, including production of functional prototypes, short-run component fabrication, component repair, and fabrication of functionally-graded materials.

Laser additive manufacturing is particularly attractive for the fabrication of titanium aerospace components because it can greatly reduce the buy-to-fly ratio and lead time for production, two factors which impact cost. Thus, a number of recent efforts have been undertaken to develop titanium laser-additive-manufacturing processes [1,2,3,4,5]. Much of the focus of this prior research has been on equipment development and mechanical property measurements [1,2]. Acceptable processing parameters have been determined largely through trial-and-error approaches. On the other hand, only limited work has been done to establish the relationship between process parameters and the structure of deposits [3,4,5]. Such an understanding is critical for both process design and control.

The work reported here is part of a larger effort to establish the effect of process parameters and input materials on deposit structure, texture, and mechanical properties. The results of efforts to characterize the effect of process parameters on structure have been described elsewhere [4,5]. The results of an initial investigation of mechanical properties in bulk Ti-6Al-4V deposits formed using the LENS™ process are described here with a focus on the relationship between properties and structure.

Materials and Procedures

Materials: The materials used in this investigation consisted of gas-atomized prealloyed Ti-6Al-4V powder made by Crucible Research and 13.23-mm-thick hot-rolled Ti-6Al-4V plate with an equiaxed-alpha microstructure. The powder had a composition (in weight percent) of 6.24 aluminum, 3.92 vanadium, 0.104 oxygen, 0.006 hydrogen, 0.007 nitrogen, 0.038 carbon, 0.047 iron, balance titanium and a mesh size of -100, +325 (particle sizes between 45 and 150 μm). The plate had a composition (in weight percent) of 6.19 aluminum, 3.89 vanadium, 0.20 oxygen, 0.0074 hydrogen, 0.01 nitrogen, 0.02 carbon, 0.12 iron, balance titanium. Prior to deposition, the plate was lapped on both sides to a surface finish of 12 to 14 μm and degreased using acetone and alcohol.

Test Material Fabrication: Two 76 mm x 76 mm x 76 mm cubes were formed in a LENS™ system using the powder and substrate material described in the previous section and the operating parameters recommended by the system manufacturer. One cube was stress relieved in vacuum for 2 hours at 700 - 730°C, while the other cube was hot isostatically pressed (HIP'ed) for 2 hours at 900°C and 100 MPa. Six cylindrical dogbone tension specimens (total length = 76 mm; gauge length = 13.5 mm; gauge diameter = 5 mm) and two ASTM E 399 compact tension specimens were extracted from each cube in each of the three primary deposition directions (Figure 1).

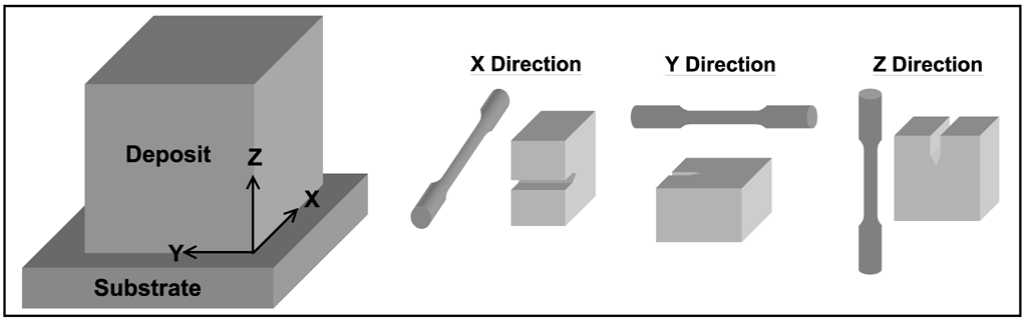

Figure 1. Illustration of the deposit geometry and the corresponding primary deposition and test-specimen directions.

Material Characterization: Remnants from each cube were sectioned, mounted, and polished using standard metallographic preparation techniques. The macrostructures and microstructures were characterized via light microscopy to assess the extent of porosity, the prior-beta grain morphology and grain size, and the morphology and scale of the transformed-beta microstructure. The crystallographic texture of the Ti-6Al-4V material produced via LENS™ was measured at a distance of approximately 6 mm from the substrate-deposit interface. It was determined using a scanning electron microscope (SEM) equipped with an electron-backscatter-diffraction (EBSD) analysis system [6].

Mechanical Testing: Standard tension tests were performed on three of the six dogbone specimens from each direction in each cube to determine the tensile yield and ultimate stresses, total elongation, and elastic modulus. The remaining dogbone specimens were used to perform fatigue tests for use in constructing an S-N fatigue curve. The compact tension specimens were used to determine fracture toughness values (i.e., $K_{I,C}$ or K_q). The fracture surfaces of all of the specimens were examined to establish the gross failure modes.

Data Analysis: The measured mechanical properties were analyzed to determine differences between different material conditions (i.e., stress-relieved vs. HIP'ed) and test directions (X, Y, and Z). The resulting tension data were also compared to published A-basis design properties for wrought, mill-annealed Ti-6Al-4V plate [7], while the fatigue and fracture-toughness data were compared to published scatterbands for cast and for wrought Ti-6Al-4V product forms [8]. Similarities and/or differences were reconciled based on the observed microstructures and texture.

Results

Microstructure/Texture: Both the stress-relieved material and the HIP'ed material contained columnar prior-beta grains with a grain size of approximately 155 μm (Figure 2a,b). A macroscopic banding (similar to that observed in previous Ti-6Al-4V material produced via LENS™ [4]) was also evident in both materials. However, the stress-relieved material contained significant lack-of-fusion porosity while the HIP'ed material contained none. This result indicated that the selected processing conditions did not produce fully consolidated material, but that porosity which did form was closed to the surface and therefore healed during HIP.

Both materials also possessed a Widmanstätten transformed-beta microstructure (Figure 2c,d); however the alpha laths in the stress-relieved material were finer than those in the HIP'ed material. This difference was expected because the higher temperature used during HIP allows the alpha phase to coarsen, while the lower temperature used for stress relief does not. Such a difference in coarseness of the alpha phase would be expected to have a noticeable effect on mechanical properties, particularly tensile strength [8].

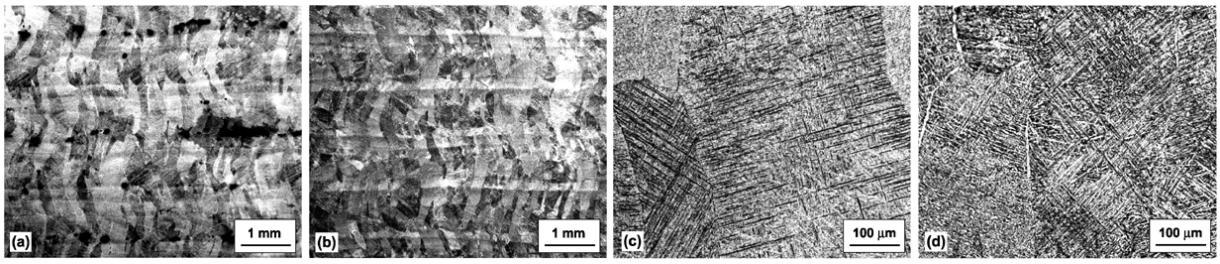

Figure 2. Photographs showing the (a,b) macrostructures and (c,d) microstructures of the (a,c) stress-relieved and (b,d) HIP'ed deposits.

The measured crystallographic texture was consistent with that which would form as a result of epitaxial growth of *columnar* beta grains from the substrate (i.e., showing the influence of both a solidification-induced <100> fiber texture and the texture of the beta-annealed substrate), However, the texture was found to be relatively weak (i.e., maximum of 2.5 times random in the alpha phase) [10].

Static Tension Test Results: The tension-test results provided insight into the effect of the deposition process and post-deposition HIP on mechanical properties (Table 1). For example, the deposits exhibited significant yield-strength anisotropy in both the stress-relieved and the HIP'ed conditions. The X- and Y-direction yield strengths were higher than those in the Z direction. However, this anisotropy was much greater in the stress-relieved condition than following HIP.

Table 1. Average Tensile Properties of Bulk Ti-6Al-4V Produced via the LENS™ Process.

Condition	Test Direction	Yield Strength (MPa)	Ultimate Strength (MPa)	Total Elongation (%)	Elastic Modulus (GPa)
Stress Relieved	X	1065	1109	4.9	116
Stress Relieved	Y	1066	1112	5.5	116
Stress Relieved	Z	832	832	0.8	112
HIP'ed	X	946	1005	13.1	118
HIP'ed	Y	952	1007	13.0	118
HIP'ed	Z	899	1002	11.8	114

The large anisotropy in the stress-relieved deposit was a direct result of the distribution of lack-of-fusion porosity in the material. Due to the layered nature of the LENS™ process, lack-of-fusion porosity tended to form primarily along the *planar* inter-layer boundaries (Figure 2a). Hence, the effective load-bearing area in tension tests perpendicular to the layer boundaries was significantly reduced, and the measured yield stress (which assumes full-density material) was correspondingly reduced. While additional lack-of-fusion porosity can also form at the inter-line boundaries *within* each layer, such porosity appeared to occur less frequently (Figure 2a). Additionally, because the line direction was alternated by 90º with each subsequent layer, inter-line porosity would be expected to have been distributed more evenly throughout the deposit and therefore have had a much smaller effect on strength. The amount of porosity and deformation observed in the fractured specimens (Figure 3) supported these conclusions. While the X- and Y-direction specimens exhibited large amounts of deformation and little porosity, the Z-direction specimens exhibited very little deformation and extensive porosity. The relative ductility of each of the three directions was further illustrated by the relative values of ultimate strength and total elongation in Table 1. While the X and Y directions had significant differences between their yield and ultimate stresses and had approximately 5% total elongation, the Z direction had no measurable difference between its yield and ultimate stresses and less than 1% total elongation.

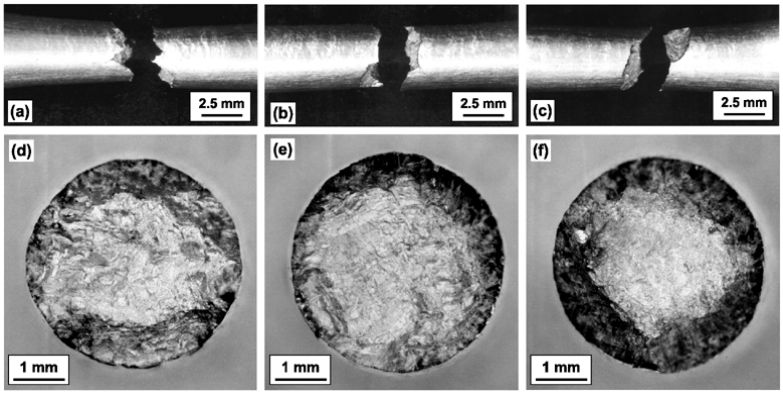

Figure 3. Macrographs of (a,b,c) broken specimens and (d,e,f) fracture surfaces of tension-test specimens cut from the stress-relieved deposit in the (a,d) X direction, (b,e) Y direction, and (c,f) Z direction.

Because the HIP'ed deposit was essentially porosity free (Figure 2b), a much smaller yield-strength anisotropy was observed. The specimens from all three directions exhibited significant ductility, as illustrated by the large amount of deformation observed in the fractured specimens (Figure 4) and the large, similar values of ultimate strength and total elongation. Hence, the yield-strength anisotropy is most likely *not* a result of porosity which might have remained incompletely healed after HIP. Instead, it is probably due to some form of mechanical

or crystallographic texture. While further research is required to determine the precise effect of various forms of texture on properties, some general comments can be made. One potential cause of the observed anisotropy is the mechanical texture due to the columnar grain morphology. In lamellar titanium microstructures, the effective slip length (which has a large, inverse effect on yield strength) is determined by the alpha colony size which, in turn, is limited by the prior-beta grain size [10]. In a columnar microstructure, the effective grain size is much smaller in directions perpendicular to the columnar grains than in the direction parallel to them. Hence, one would expect the yield strength to be lower in the direction parallel to the columnar grains (which in this case is the Z direction). Another possible cause of anisotropy is crystallographic texture [11]. Due to the high anisotropy of the hexagonal crystal structure, texture can greatly affect mechanical properties in titanium alloys. Because the texture of Ti-6Al-4V LENS™ deposits is markedly affected by the <100> fiber texture which forms during columnar solidification, a difference in texture between the Z direction and the X and Y directions would be expected and was indeed observed [9]. However, the effect of this texture on properties is not straightforward and requires further investigation.

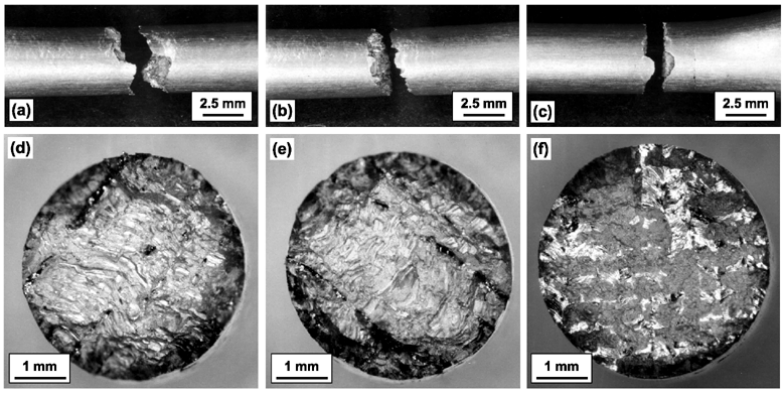

Figure 4. Macrographs of the (a,b,c) broken specimens and (d,e,f) fracture surfaces of tension-test specimens cut from the HIP'ed deposit in the (a,d) X direction, (b,e) Y direction, and (c,f) Z direction.

Another interesting observation was the significant difference in strength and ductility for the stress-relieved and HIP'ed material conditions. Focussing on the X- and Y-direction results, the stress-relieved material was stronger yet less ductile than the HIP'ed material. The difference in strength was likely a result of the difference in alpha-platelet thickness between the two materials with the coarser HIP'ed material being weaker. The difference in ductility was probably due to the presence of porosity in the stress-relieved material.

The Z-direction tension properties of these materials showed interesting comparisons to published design properties for wrought, mill-annealed Ti-6Al-4V (Table 2). While the strength and ductility of the stress-relieved material were severely limited by porosity, the yield strength was not particularly low when compared to the wrought material. Considering the much higher strengths and ductilities observed in the X and Y directions, it appears that the LENS™ process actually may offer improvements in tensile strength provided that the material can be fabricated *without* porosity. However, even if HIP is required to heal porosity, a modest improvement in strength relative to wrought properties can be achieved without a significant loss of ductility.

Table 2. Measured Z-Direction Tension Properties of Bulk Ti-6Al-4V Produced via the LENS™ Process versus Published A-Basis Design Properties for Wrought, Mill-Annealed Ti-6Al-4V Plate [7].

Condition	Yield Strength (MPa)	Ultimate Strength (MPa)	Total Elongation (%)	Elastic Modulus (GPa)
Stress Relieved	832	832	0.8	112
HIP'ed	899	1002	11.8	114
Wrought	827	896	10	110

Tensile Fatigue Test Results: The tensile fatigue test results revealed the expected trends in view of the distribution of porosity in the deposits (Figure 5). The stress-relieved material had much lower fatigue strengths than the HIP'ed material and also displayed an anisotropy. The Z-direction fatigue strengths were significantly lower than those in the X and Y directions. When compared to alternate product forms, the fatigue strength of the HIP'ed material was similar to that of wrought product, indicating that no debit in fatigue strength would need to be considered in component design.

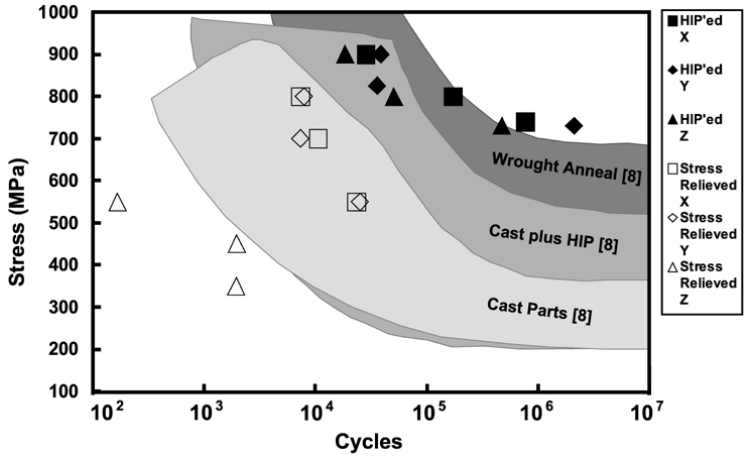

Figure 5. Comparison of measured fatigue strengths for Ti-6Al-4V deposits in both the stress-relieved and HIP'ed conditions to published scatterbands for Ti-6Al-4V castings and forgings (Reference 8).

Compact Tension Test Results: The compact tension results further demonstrated the effect of lack-of-fusion porosity on mechanical behavior. In the stress-relieved specimens, a strong anisotropy was again observed (Figures 6 and 7). In the X-direction specimens (Figure 6a,d), the crack did not begin at the notch tip, but instead at the nearest layer of lack-of-fusion porosity. From there, the crack grew rapidly with little plastic deformation thus resulting in a very low fracture toughness (Figure 7). In the Y and Z directions, the porosity layers were not in the same plane as the crack; thus, larger fracture toughnesses were obtained (Figure 7). In addition, an unusual phenomenon occurred in the Z-direction specimens (Figure 6c,f). The crack propagated along the original plane for a significant distance and then began to propagate along the layers of porosity at an angle 90° from the original plane. Nevertheless, these specimens exhibited the *highest* toughness values for the stress-relieved material (Figure 7).

In contrast, the HIP'ed specimens exhibited a much smaller level of anisotropy (Figures 7 and 8). The Z-direction toughness was slightly higher than that for the other directions. Significant ductility and nominally planar cracks were observed in all three directions (Figure 8).

Hence, the cause of the observed anisotropy is likely related to the same source as the observed yield-strength anisotropy.

Finally, upon comparing the toughness of these materials to those of other product forms, the toughness of the stress-relieved material fell below published values for wrought and cast product forms, while that of the HIP'ed material lay within the range of published values.

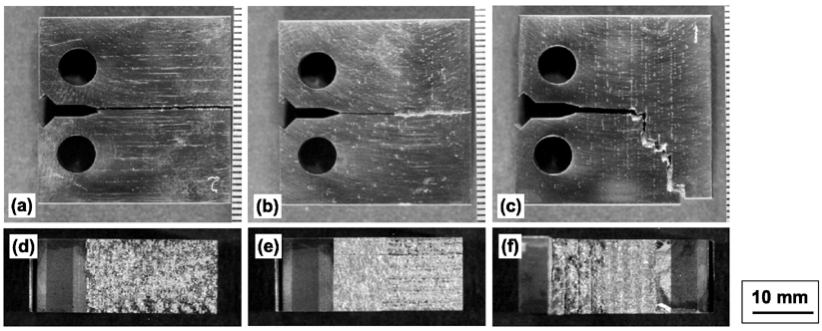

Figure 6. Macrographs showing the (a,b,c) broken specimens and (d,e,f) fracture surfaces of the compact-tension specimens from the stress-relieved deposits in the (a,d) X direction, (b,e) Y direction, and (c,f) Z direction.

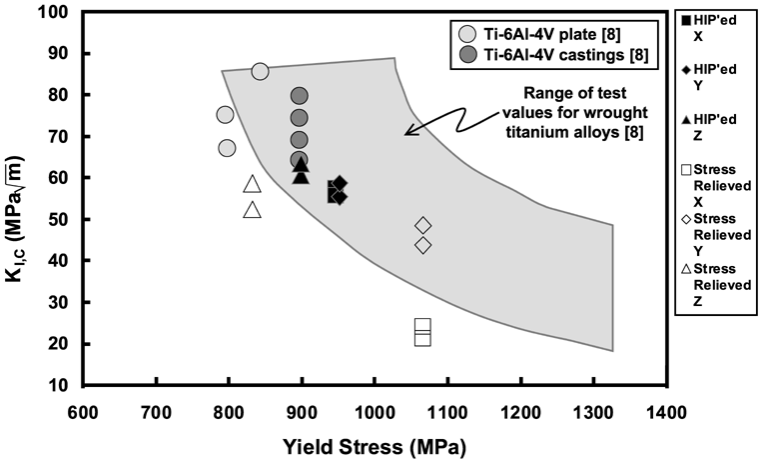

Figure 7. Comparison of measured $K_{I,C}$ and yield-strength values for Ti-6Al-4V deposits in both the stress-relieved and HIP'ed conditions to a published scatterband for wrought Ti-6Al-4V (Reference 8).

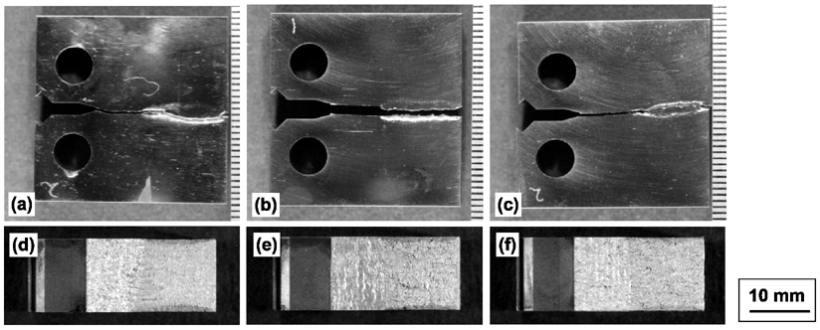

Figure 8. Macrographs showing the (a,b,c) broken specimens and (d,e,f) fracture surfaces of the compact-tension specimens from the HIP'ed deposits in the (a,d) X direction, (b,e) Y direction, and (c,f) Z direction.

Summary and Conclusions

The effect of microstructure and texture of laser-deposited Ti-6Al-4V on mechanical properties was investigated by conducting tension, fatigue, and fracture toughness tests. From this work, the following conclusions were drawn:

1. Lack-of-fusion porosity has a significant effect on both the levels and anisotropy of mechanical properties.
2. HIP appears to be effective in healing lack-of-fusion porosity.
3. The yield strength can show a noticeable anisotropy due to residual deposition porosity (in the stress-relieved condition) and mechanical and/or crystallographic texture (in both conditions).
4. The static tensile strength and ductility, fatigue strength, and fracture toughness of HIP'ed Ti-6Al-4V produced via LENS™ compare favorably to those of wrought products.

Acknowledgements

This work was conducted as part of the in-house research activities of the Metals Processing Group of the Air Force Research Laboratory's Materials and Manufacturing Directorate. The support and encouragement of the Laboratory management and the Air Force Office of Scientific Research (Dr. C.S. Hartley, program manager) are gratefully acknowledged. The assistance of P. Gorman of Optomec Design Co. and W. Capshaw of ICE Prototyping in fabricating the deposits, D. Maxwell in performing the mechanical tests, S. Short, J. Vann, and R. Lewis in preparing and analyzing the metallographic specimens, and M. Glavicic in performing the OIM analysis is also much appreciated.

References

[1] Schriempf, J.T., Whitney, E.J., Blomquist, P.A., Arcella, F.G., *Advances in Powder Metallurgy and Particulate Materials*, v. 3, Princeton, NJ: Metal Powder Industries Federation, 1997:21-51.
[2] Keicher D.M., Miller, W.D., *Hard Coatings Based on Borides, Conference: Carbides & Nitrides: Synthesis, Characterization & Applications*, San Antonio, TX, USA, 16-19 Feb. 1998, Warrendale, PA: TMS, 1998: 369.
[3] Brice, C.A., Schwendner, K.I., Mahaffey, D.W., Moore, E.H., Fraser, H.L., *Proceedings of the 10th Solid Freeform Fabrication Symposium*, University of Texas at Austin, Austin, TX, USA, Aug. 1999.
[4] Kobryn, P.A., Moore, E.H., and Semiatin, S.L., *Scripta Materialia*, v. 43, no. 4, 2000.
[5] Kobryn, P.A. and Semiatin, S.L., *Proceedings of the 11th Solid Freeform Fabrication Symposium*, University of Texas at Austin, Austin, TX, USA, Aug. 2000.
[6] Adams, B.L., Wright, S.I., and Kunze, K., *Metall. Trans. A*, v. 24A, 1993: 819.
[7] MIL-HDBK-5H, Battelle's Columbus Labs, Columbus, OH, 1998.
[8] Donachie, M. J. Jr., ed., *Titanium: A Technical Guide*, ASM International, 1988.
[9] Kobryn, P.A., Glavicic, M.G., and Semiatin, S.L., AeroMat 2001, Long Beach, CA, June 13th, 2001.
[10] Lütjering, G., *Mater. Sci. Eng. A*, v. A243, 1998: 32.
[11] Williams, J.C. and Starke, E.A. Jr., in: G. Krauss, ed., *Deformation, Processing, and Structure*, ASM, 1984: 279.